

# Detecting intrinsic scattering changes correlated to neuron action potentials using optical coherence imaging

Benedikt W. Graf,<sup>1</sup> Tyler S. Ralston<sup>1</sup>, Han-Jo Ko,<sup>1</sup>  
and Stephen A. Boppart<sup>\*1,2</sup>

Biophotonics Imaging Laboratory  
Beckman Institute for Advanced Science and Technology  
<sup>1</sup> Department of Electrical and Computer Engineering,  
<sup>2</sup> Department of Bioengineering, Department of Medicine  
University of Illinois at Urbana-Champaign  
405 N. Mathews Avenue, Urbana, IL 61801  
[\\*boppart@illinois.edu](mailto:*boppart@illinois.edu)

**Abstract:** We demonstrate how optical coherence imaging techniques can detect intrinsic scattering changes that occur during action potentials in single neurons. Using optical coherence tomography (OCT), an increase in scattering intensity from neurons in the abdominal ganglion of *Aplysia californica* is observed following electrical stimulation of the connective nerve. In addition, optical coherence microscopy (OCM), with its superior transverse spatial resolution, is used to demonstrate a direct correlation between scattering intensity changes and membrane voltage in single cultured *Aplysia* bag cell neurons during evoked action potentials. While intrinsic scattering changes are small, OCT and OCM have potential use as tools in neuroscience research for non-invasive and non-contact measurement of neural activity without electrodes or fluorescent dyes. These techniques have many attractive features such as high sensitivity and deep imaging penetration depth, as well as high temporal and spatial resolution. This study demonstrates the first use of OCT and OCM to detect functionally-correlated optical scattering changes in single neurons.

©2009 Optical Society of America

**OCIS codes:** (170.4500) Optical coherence tomography; (170.2655) Functional monitoring and imaging.

---

## References and links

1. M. A. Nicoletis, and S. Ribeiro, "Multielectrode recordings: the next steps," *Curr. Opin. Neurobiol.* **12**(5), 602–606 (2002).
2. B. J. Baker, E. K. Kosmidis, D. Vucinic, C. X. Falk, L. B. Cohen, M. Djuricic, and D. Zecevic, "Imaging brain activity with voltage- and calcium-sensitive dyes," *Cell. Mol. Neurobiol.* **25**(2), 245–282 (2005).
3. D. K. Hill, and R. D. Keynes, "Opacity changes in stimulated nerve," *J. Physiol.* **108**, 278–281 (1949).
4. L. B. Cohen, R. D. Keynes, and D. Landowne, "Changes in axon light scattering that accompany the action potential: current-dependent components," *J. Physiol.* **224**(3), 727–752 (1972).
5. L. B. Cohen, R. D. Keynes, and B. Hille, "Light scattering and birefringence changes during nerve activity," *Nature* **218**(5140), 438–441 (1968).
6. R. A. Stepnoski, A. LaPorta, F. Raccuia-Behling, G. E. Blonder, R. E. Slusher, and D. Kleinfeld, "Noninvasive detection of changes in membrane potential in cultured neurons by light scattering," *Proc. Natl. Acad. Sci. U.S.A.* **88**(21), 9382–9386 (1991).
7. K. Holthoff, and O. W. Witte, "Intrinsic optical signals in rat neocortical slices measured with near-infrared dark-field microscopy reveal changes in extracellular space," *J. Neurosci.* **16**(8), 2740–2749 (1996).
8. R. U. Maheswari, H. Takaoka, R. Homma, H. Kadono, and M. Tanifuji, "Implementation of optical coherence tomography (OCT) in visualization of functional structures of cat visual cortex," *Opt. Commun.* **202**(1-3), 47–54 (2002).
9. R. U. Maheswari, H. Takaoka, H. Kadono, R. Homma, and M. Tanifuji, "Novel functional imaging technique from brain surface with optical coherence tomography enabling visualization of depth resolved functional structure *in vivo*," *J. Neurosci. Methods* **124**(1), 83–92 (2003).

10. U. M. Rajagopalan, and M. Tanifuji, "Functional optical coherence tomography reveals localized layer-specific activations in cat primary visual cortex *in vivo*," *Opt. Lett.* **32**(17), 2614–2616 (2007).
11. A. D. Aguirre, Y. Chen, J. G. Fujimoto, L. Ruvinskaya, A. Devor, and D. A. Boas, "Depth-resolved imaging of functional activation in the rat cerebral cortex using optical coherence tomography," *Opt. Lett.* **31**(23), 3459–3461 (2006).
12. T. Akkin, D. P. Dave, T. E. Milner, and H. Rylander Iii, "Detection of neural activity using phase-sensitive optical low-coherence reflectometry," *Opt. Express* **12**(11), 2377–2386 (2004).
13. C. Fang-Yen, M. C. Chu, H. S. Seung, R. R. Dasari, and M. S. Feld, "Noncontact measurement of nerve displacement during action potential with a dual-beam low-coherence interferometer," *Opt. Lett.* **29**(17), 2028–2030 (2004).
14. T. Akkin, C. Joo, and J. F. de Boer, "Depth-resolved measurement of transient structural changes during action potential propagation," *Biophys. J.* **93**(4), 1347–1353 (2007).
15. M. Lazebnik, D. L. Marks, K. Potgieter, R. Gillette, and S. A. Boppart, "Functional optical coherence tomography for detecting neural activity through scattering changes," *Opt. Lett.* **28**(14), 1218–1220 (2003).
16. X. C. Yao, A. Yamauchi, B. Pery, and J. S. George, "Rapid optical coherence tomography and recording functional scattering changes from activated frog retina," *Appl. Opt.* **44**(11), 2019–2023 (2005).
17. K. Bizheva, R. Pflug, B. Hermann, B. Povazay, H. Sattmann, P. Qiu, E. Anger, H. Reitsamer, S. Popov, J. R. Taylor, A. Unterhuber, P. Ahnelt, and W. Drexler, "Optophysiology: depth-resolved probing of retinal physiology with functional ultrahigh-resolution optical coherence tomography," *Proc. Natl. Acad. Sci. U.S.A.* **103**(13), 5066–5071 (2006).
18. V. J. Srinivasan, M. Wojtkowski, J. G. Fujimoto, and J. S. Duker, "*In vivo* measurement of retinal physiology with high-speed ultrahigh-resolution optical coherence tomography," *Opt. Lett.* **31**(15), 2308–2310 (2006).
19. J. A. Izatt, M. R. Hee, G. M. Owen, E. A. Swanson, and J. G. Fujimoto, "Optical coherence microscopy in scattering media," *Opt. Lett.* **19**(8), 590–592 (1994).
20. L. K. Kaczmarek, and F. Strumwasser, "The expression of long lasting afterdischarge by isolated *Aplysia* bag cell neurons," *J. Neurosci.* **1**(6), 626–634 (1981).
21. D. Landowne, "Molecular motion underlying activation and inactivation of sodium channels in squid giant axons," *J. Membr. Biol.* **88**(2), 173–185 (1985).
22. F. E. Dudek, and A. Kossatz, "Conduction velocity and spike duration during afterdischarge in neuroendocrine bag cells of *Aplysia*," *J. Neurobiol.* **13**(4), 319–326 (1982).
23. P. R. Harley, "A possible age-related decrement in the conduction velocity of *Aplysia* neuron R2," *Experientia* **31**(8), 901–902 (1975).
24. J. F. de Boer, T. E. Milner, M. J. van Gemert, and J. S. Nelson, "Two-dimensional birefringence imaging in biological tissue by polarization-sensitive optical coherence tomography," *Opt. Lett.* **22**(12), 934–936 (1997).
25. B. J. Vakoc, S. H. Yun, J. F. de Boer, G. J. Tearney, and B. E. Bouma, "Phase-resolved optical frequency domain imaging," *Opt. Express* **13**(14), 5483–5493 (2005).
26. B. H. Park, M. C. Pierce, B. Cense, and J. F. de Boer, "Real-time multi-functional optical coherence tomography," *Opt. Express* **11**(7), 782–793 (2003).
27. R. Huber, D. C. Adler, and J. G. Fujimoto, "Buffered Fourier domain mode locking: Unidirectional swept laser sources for optical coherence tomography imaging at 370,000 lines/s," *Opt. Lett.* **31**(20), 2975–2977 (2006).

## 1. Introduction

Traditional methods for measuring electrical activity in individual neurons are based on making physical contact or penetrating the cell membrane with metal or glass capillary electrodes. These techniques are limited by the fact that only a few neurons can be practically observed simultaneously, and that the neurons are physically disturbed and possibly damaged. This approach is further complicated when the neurons are located in tissue. To record activity from larger populations of neurons simultaneously, multi-electrode arrays have been used [1]. However, these devices measure extracellular activity from ensembles of neurons and can be invasive. The development of techniques for optically detecting neural activity with voltage- or calcium-sensitive fluorescent dyes has enabled activity from groups of individual neurons to be detected without making physical contact [2]. This has had a profound impact on the field of neuroscience. However, using dyes has several disadvantages including difficulty in dye administration, photo-bleaching, and toxic effects which limit the applications of such techniques. Neuroscience would greatly benefit from non-invasive, non-contact, label-free methods of detecting neural activity from single neurons.

It has been known for decades that a change in the membrane potential in neural tissue is accompanied by a change in the intrinsic optical properties [3]. Various techniques have been utilized in order to detect these optical effects and correlate them to electrical activity. Early experiments relied on measuring changes in the polarization and intensity of transmitted light in squid giant axons [4] and crab nerve fibers [5]. Dark field microscopy, which features an increased sensitivity to small changes in scattering, has been demonstrated in a number of

studies [6,7] While several optical imaging techniques have been used, more sensitive detection methods are in demand. Optical coherence tomography (OCT) is an emerging imaging modality that measures backscattered light in biological tissue with a sensitivity exceeding 100 dB. OCT is analogous to ultrasound imaging in that the depth-resolved scattering information is obtained by sending a wave into the sample and measuring the time delay of reflected waves from scatterers. OCT combines high spatial and temporal resolution with the ability to image several millimeters into intact tissue samples. These features make OCT a potentially attractive tool for detecting electrical activity in neural tissue for investigations in neuroscience.

While intrinsic optical signals are inherently small and often difficult to reliably detect, recent research has demonstrated the feasibility of OCT and related techniques for measuring functional activity in various tissue types. OCT has been used to map changes in scattering in a cat cortex in response to a visual stimulus [8–10]. Recently, changes in scattering intensity from rat cortex in response to electrical stimulation was observed using OCT [11]. Phase-sensitive low-coherence imaging techniques have been used to detect nerve displacements in response to action potentials in crayfish [12] and lobster [13] nerve bundles. Depth-dependent scattering changes in response to electrical stimulation in crayfish nerve bundles [14] and *Aplysia* nerve fibers [15] using OCT have also been reported. Detection of increased scattering changes from photoreceptors in animal retina due to a visual stimulus has been demonstrated both *ex vivo* [16,17] and *in vivo* [18].

While past research has demonstrated the detection of neural activity using optical coherence imaging techniques, these studies focused on large populations of neurons or nerve fiber bundles. In this study, we utilize OCT and a high resolution variation called optical coherence microscopy (OCM) to detect scattering changes in single neurons that are correlated to induced electrical activity. OCT is used to detect scattering changes over a large depth of field from *in situ* neurons in the abdominal ganglion of *Aplysia californica*. OCM, with higher spatial resolution [19], is demonstrated on single *Aplysia* bag cell neurons in culture to show a direct relationship between membrane voltage and scattering intensity. Both OCT and OCM have potential applications as tools for non-invasive, non-contact, and label-free measurements of functional activity in neurons. In addition, these techniques could also be used to further understand the contribution of individual neurons to functionally correlated changes in macroscopic optical properties of neural tissue.

## 2. Materials and methods

### 2.1 Neurons from *Aplysia californica*

Large juvenile *Aplysia californica* (80-100 gram) were obtained from the NIH National Resource for *Aplysia* at the University of Miami and housed in a salt water aquarium for no more than two weeks before experiments. *Aplysia* were first euthanized with an injection of 40-60 ml of 390 mM magnesium chloride ( $MgCl_2 \cdot 6H_2O$ ). Abdominal ganglia were dissected out and placed in a beaker of Artificial Sea Water (ASW). For *in situ* OCT imaging, a whole ganglion was placed in a culture dish with ASW as the media. For *in vitro* OCM imaging, individual bag cell neurons from the abdominal ganglion were cultured. The ganglia were first treated for 90-120 minutes at 35 °C with an enzyme solution (100  $\mu$ g type XIV protease in 1 ml ASW) to soften the connective tissue. Individual bag cell neurons were micro-dissected from the treated ganglia and transferred to a separate culture dish containing ASW and a 1% antibiotic solution (A5955, Sigma-Aldrich, St. Louis, MO). Cells were then incubated at 14 °C for 1-2 days before experimental use.

### 2.2 Electrophysiology

Electrical stimulation and recording of neuron activity was performed differently for the *in vitro* and *in situ* preparations. For stimulation and recording from neurons *in situ*, two suction electrodes were used, attached to two different locations on the abdominal ganglion. One electrode was used to stimulate the fiber while the other recorded the compound action

potentials. Stimulation in this manner periodically resulted in a compound action potential. Accordingly, acquisition of optical data was not synchronized to the stimulation. Changes in optical scattering recorded during an action potential were analyzed for correlations.

For the *in vitro* preparation single sharp glass micro-pipettes filled with 3M KCl were used to stimulate the cultured neurons and simultaneously record the membrane voltage. The micro-pipettes were mounted on a headstage (HS-2A, Axon Instruments, SunnyVale, CA) and connected to an electrophysiology amplifier (GeneClamp 500B, Axon Instruments, SunnyVale, CA). The amplifier was connected to a PC via a 16-bit digitizer (Digidata 1322A Axon Instruments, Sunny Vale, CA). Stimulation and recording was controlled using electrophysiology data acquisition software (Clampex, Axon Instruments, SunnyVale, CA). Direct cable connections to the optical coherence imaging setups were used to synchronize electrical and optical measurements.

### 2.3 Optical coherence imaging

A general schematic of a spectral domain optical coherence imaging system is shown in Fig. 1. The broadband laser source is split by a beam splitter into the reference and sample arm. Light reflected from the sample arm and the reference arm is combined and spectrally-dispersed onto to a line scan camera. The depth-dependent scattering profile of the sample is obtained by taking the inverse Fourier transform of the interference pattern imaged by the camera. To visualize the structure of the sample, the laser beam is scanned by a pair of mirrors mounted on computer-controlled galvanometers during acquisition. In OCT the resulting cross-sectional image is called a brightness mode (B-mode) image. In OCM, where essentially only one depth has high lateral resolution, images are acquired in the *en face* plane. To measure time-dependent scattering changes from one axial scan, the beam is held stationary while data is acquired over time. The resulting image is known as a motion mode (M-mode) image.

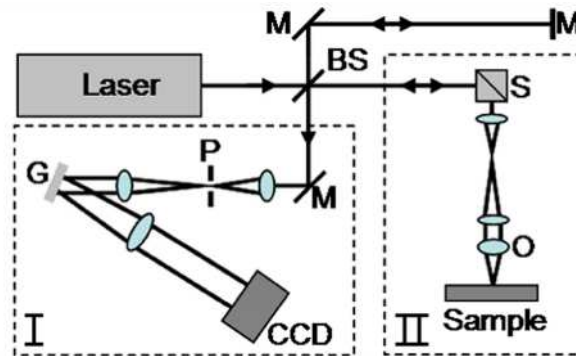


Fig. 1. Schematic of a free-space spectral-domain OCT/OCM system. The output of the laser is split into the reference arm and the sample arm (region II). The combined reflections from the reference and sample arm are detected by the spectrometer (region I) giving a depth profile of the sample. The scanning mirrors move the beam across the sample to construct an image. (BS) beamsplitter, (M) mirror, (P) pinhole, (G) diffraction grating, (CCD) CCD line camera, (S) scanning mirrors, (O) objective.

The OCT setup for this experiment was a fiber-based system with a Ti-Sapphire laser centered at 800 nm with ~100 nm bandwidth. This corresponds to a 3 micrometer axial resolution. The sample arm consisted of a collimating lens, two galvanometer-driven mirrors to scan the beam in the x and y directions and a 0.05 NA lens to focus the beam onto the sample. The beam diameter at the focus and thus the transverse resolution was roughly 10 micrometers. The free-space spectrometer used for data acquisition utilized a 1200 lines/mm grating and a 2048 element line scan camera (P2-22-02K40, Dalsa). Scanning of the beam and data acquisition was synchronized using a PC running custom software.

The OCM setup was a free-space system using a tunable Ti-Sapphire laser with a bandwidth of  $\sim 10$  nm. The sample arm for this setup was an upright microscope (BX61WI, Olympus) with a 0.25 NA, 10X objective (MPLN10X, Olympus) with a micro-positioning stage (MTP-3500-00, Scientifica) to hold the sample. The confocal parameter of this objective as well as the coherence length in free space of this source are both roughly  $30\ \mu\text{m}$ . The laser beam was directed to the sample through a port in the back of the microscope. This setup allows for simultaneous OCM imaging and electrophysiological measurements. The same spectrometer from the OCT setup was used for these OCM studies. Data acquisition and processing was done with a PC running LabVIEW software.

### 3. Results

#### 3.1 Optical coherence tomography for detecting depth-resolved scattering changes caused by electrical activity

Figure 2(A) shows a light microscope image of the abdominal ganglion from an *Aplysia californica* pinned in a dish filled with ASW. The dish was placed in the sample arm of the OCT system. The red lines in Fig. 2(A) indicate the orientation of the cross-sectional B-mode OCT images of the ganglion shown in Fig. 2(B,D). Individual neurons are clearly visible in the OCT images and the specific neurons are numbered in both the light microscope (Fig. 2(A)) and the OCT images (Fig. 2(B,D)). By positioning the OCT beam at a stationary point on a neuron of interest (red arrow in Fig. 2(B)), the depth-resolved, time-dependent changes in scattering from a specific neuron can be observed. Figure 2(C) shows an M-mode image representing the scattering versus depth over a period of several seconds from neuron #2. No electrical activity in the neuron was induced or recorded during this measurement. The scattering changes observed are natural fluctuations in scattering possibly caused by movement of sub cellular scatterers or cytoplasmic streaming. Figure 2 simply demonstrates the ability of OCT to image a population of neurons, select a specific neuron of interest and then observe changes in scattering throughout the depth of that neuron over a period of time. This approach enables high resolution detection of scattering changes of neurons in the ganglion.

To observe the changes in scattering that are correlated to electrical activity, M-mode images were taken from the R14 (not seen in Fig. 2) neuron near the branchial nerve. The neuron was stimulated with a bi-polar electrode placed near the cell, while a second suction electrode placed on the end of the nerve fiber simultaneously recorded the voltage. The stimulus waveform was a 100 Hz, 2 V square wave. OCT data was acquired from a single point at a 2 kHz line rate (one depth scan every  $500\ \mu\text{s}$ ) during stimulation. Figure 3 shows the scattering from the entire depth of the neuron displayed in a motion mode (M-mode) image that was acquired during the detection of an action potential (recorded electrical trace shown at bottom of image). In this M-mode image the changes in scattering were emphasized by subtracting the background. The background was obtained by acquiring an M-mode image during a period of no stimulation and averaging all the axial scans. Subtracting this averaged axial scan from each column of the M-mode image during stimulation highlights changes caused by the electrical activity. A slow increase in scattering intensity is apparent in the neuron following the action potential. Because the electrical recording is a compound action potential the observed optical activity is not expected to follow the time course of the electrophysiology. To more clearly demonstrate the changes in light scattering from single neurons in response to its electrical activity, and to eliminate the potential cross-talk that may occur from neurons located *in situ* within the abdominal ganglion, individual cultured neurons were investigated.

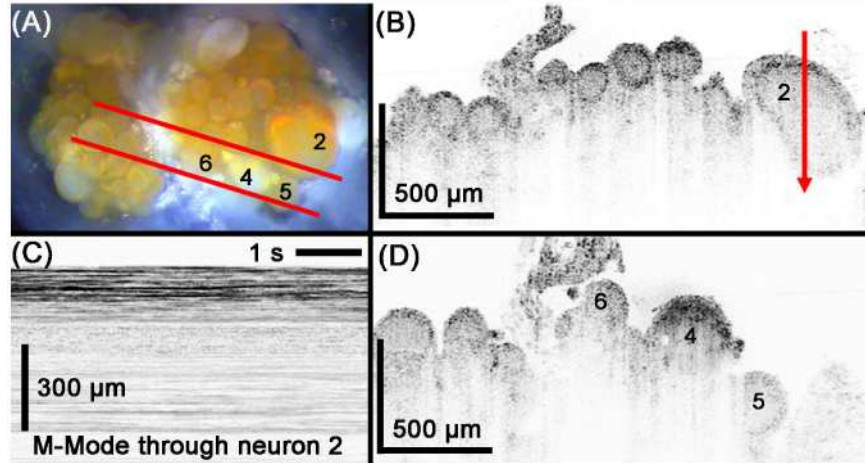


Fig. 2. Depth-resolved optical scattering changes over time from a single neuron *in vitro*. (A) Stereo microscope view of the *Aplysia* abdominal ganglion. (B,D) B-mode OCT images acquired from the ganglion. Orientation of B-mode images is shown by the red lines in (A). Numbers indicate specific neurons seen in the microscope image and the OCT images. (C) M-mode image showing the scattering over time from one position of the B-mode image, as indicated by the red arrow in (B).

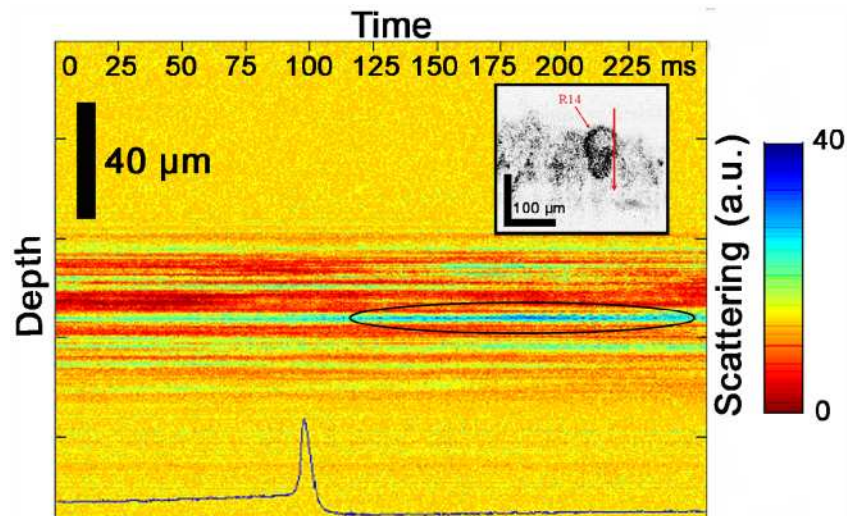


Fig. 3. M-mode image from a point on the *in situ* R14 cell during stimulation of the ganglion. Blue trace overlaying the M-mode image shows the action potential recorded by the electrode. An increase in scattering after the action potential from one depth is indicated by the black oval.

### 3.2 Optical coherence microscopy for single cell membrane voltage and scattering correlation

A direct correlation between the scattering intensity and membrane voltage required that the membrane voltage be directly measured using a glass micro-pipette electrode. Also, because the natural fluctuations in scattering caused by other neurons in the ganglion could potentially contribute to the optical responses that were recorded in Fig. 3, individual cultured neurons were investigated. OCM was used instead of OCT because it offers a higher transverse resolution and sensitivity, allowing for the detection of scattering changes from specific regions of the neuron.

Figure 4 shows an *en face* OCM image of a cultured bag cell neuron from the abdominal ganglion. The red arrow in the image indicates the location of the beam during M-mode OCM imaging. This site was chosen because the axon hillock has the highest density of ion channels and thus is where the highest optical response was expected. A micro-pipette electrode was inserted into the body of the neuron and a reference lead was placed in the cell bath. Stimulation of the neuron was done with 10 nA current pulses 250 ms in duration at a rate of 2 per second. Simultaneous recording of the membrane voltage was done with the same electrode. The induced action potentials (the spike in membrane voltage following the onset of the stimulus) were roughly 50 ms in duration at half amplitude. This duration is expected for a preparation of cultured *Aplysia* bag cell neurons when repeatedly stimulated [20].

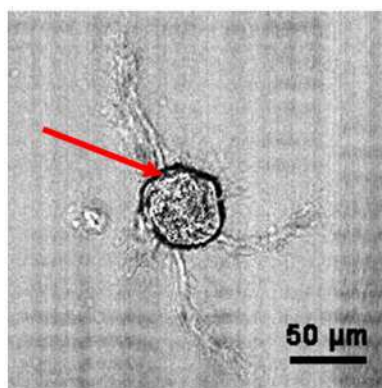


Fig. 4. *En face* OCM image of a single cultured *Aplysia* bag cell neuron. The high transverse resolution offered by OCM allows individual cells to be imaged at high resolution. The red arrow points to the axon hillock, the location of M-mode image acquisition.

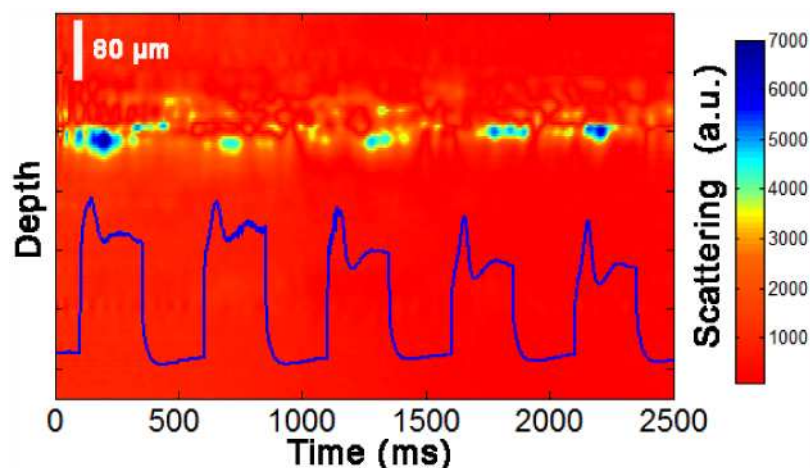


Fig. 5. M-mode scattering image and membrane voltage of a single bag cell neuron in culture during a train of stimulation pulses. Beam was positioned over the axon hillock of the neuron. Stimulation of the neuron causes an increase in the scattering intensity from the cell membrane.

OCM data from the fixed location on the neuron was acquired during electrical stimulation at a line rate of 1 kHz (one recording every 1 ms). Figure 5 shows an M-mode image from the neuron during a train of five electrical stimuli. The voltage and scattering traces are both an average of five sets of stimuli. The changes in scattering are emphasized by removing the DC background and the high frequency components above 60 Hz (attributed to background noise) from the scattering data using Fourier transform filtering. Figure 5 shows that there is an increase in scattering corresponding to each of the stimuli. Scattering in the M-mode OCM

image is limited to a small depth range because the height of the neuron at the location of recording is roughly  $35\ \mu\text{m}$  and because the small confocal parameter of the objective ( $\sim 30\ \mu\text{m}$ ) limits the recording of scattering changes to the cell volume that is within the focal volume of the objective.

Figure 6A shows an M-mode OCM image from a neuron for a single electrical stimulus. The corresponding membrane voltage is plotted with a scattering trace from a single depth in Fig. 6B. The data is for an average of 25 stimuli. The scattering data was processed in the same way as Fig. 5. The blue arrow in Fig. 6A indicates the scattering surface which corresponds to the top surface of the neuron while the scattering surface directly beneath it is the reflection from the culture dish surface. The fluctuations in scattering intensity from the culture dish are likely due to the fact that scattering changes from the neuron affect the amount of light reaching that surface. There is an apparent decrease in scattering from the culture dish that coincides with the stronger reflection from the neuron surface. The correlation between the scattering intensity and the membrane voltage demonstrate that optical coherence imaging can detect the fast changes in optical properties from single neurons, and that the spatial resolution is sufficient to localize these changes to the membranes of these cells.

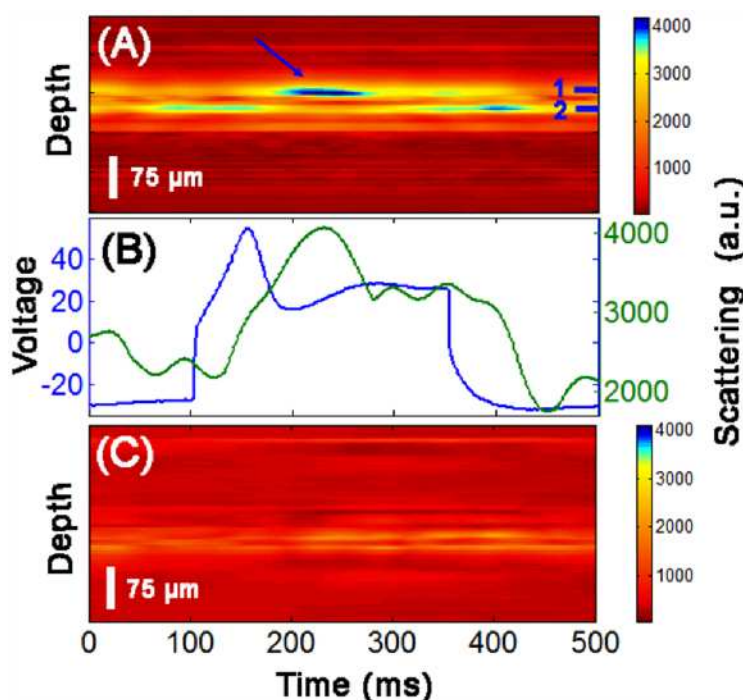


Fig. 6. Comparison between membrane voltage and scattering intensity of a neuron during a single action potential. (A) M-mode scattering image. The top surface of the neuron is indicated by position 1 while reflection from the culture dish is seen at position 2. An increase in scattering from the neuron corresponding to the action potential is indicated by the blue arrow. (B) Membrane voltage and scattering from the neuron surface for a single stimulation. Scattering intensity is shown to closely follow the time course of the membrane voltage. The blue and green traces correspond to the voltage and optical scattering signals, respectively. (C) M-mode scattering image from same neuron without stimulation.

#### 4. Discussion

We have shown that optical coherence imaging can be used to detect changes in the intrinsic optical properties of single neurons that accompany action potentials. OCT was used to observe scattering changes from neurons in the abdominal ganglion of *Aplysia californica*

during stimulation of a connective nerve. OCM, which offers higher transverse resolution, was used to show a correlation between membrane voltage and scattering intensity from single cultured *Aplysia* bag cell neurons during action potentials. The changes in scattering follow a similar time scale as the membrane voltage. Past research, as discussed in the introduction, has demonstrated the feasibility of optical coherence imaging techniques for detecting functional activity in various neural tissue types including crustacean nerve fibers, *Aplysia* ganglion, and mammalian cortex and retina. In this study, we show that these techniques have potential use for optical detection of functional activity in single neurons. In addition, this ability could serve future studies designed to better understand the origins of intrinsic scattering signals from large populations of neurons.

We demonstrated the capability of OCT to image a population of neurons and then selected a particular neuron for investigation of functional activity with M-mode imaging. M-mode imaging of a single neuron in the population showed that there are scattering changes present without electrical stimulation. We speculate that these fluctuations are caused in part by intrinsic biological processes which may include localized spontaneous electrical activity or trafficking of vesicles in the cytoplasm. Upon electrical stimulation of the ganglion, compound action potentials in the ganglion were detected and an increase in scattering from the neuron was observed. These changes were slow with respect to the measured compound action potential, which was less than 15 ms in duration (Fig. 3). The timing of the observed scattering changes indicates that swelling of the neuron is a likely mechanism. Slow optical responses in squid giant axons have been found to be caused by an influx or efflux of ions resulting in swelling or shrinking of the periaxonal space [4]. On the contrary, scattering changes which follow the time course of the electrical activity and are linearly proportional to the membrane voltage are thought to be caused by the realignment of charged molecules in the membrane of neurons [6,21]. Measurement of functional activity based on swelling due to flow of ions [17] and hemodynamic effects [11] with OCT has been previously demonstrated. In this study we have shown that OCT can detect such scattering changes from individual neurons.

While OCT allowed scattering changes to be localized to the neurons used in this study, the typical transverse resolutions in OCT (10-20  $\mu\text{m}$ ) are likely insufficient to identify smaller mammalian neurons that are often studied in neuroscience. OCM is a variation of OCT that uses higher numerical aperture optics to focus light to a smaller spot size. OCM can have a transverse resolution less than 1 micron at the expense of a short depth-of-field. We demonstrated OCM on single cultured *Aplysia* bag cell neurons to show high resolution imaging capabilities as well as to show a direct correlation between membrane voltage and optical scattering intensity during action potentials. Increases in scattering intensity from neurons were observed to followed the time course of the induced action potentials and membrane depolarization. Intrinsic optical signals that are linearly dependent on membrane voltage have been observed in previous studies [5,21]. One mechanism of these optical signals is believed to be a realignment of charged membrane proteins in response to a voltage change [6]. With the correlation between the membrane voltage and the scattering changes observed in this study, it is likely that the realignment of membrane proteins is the dominant mechanism.

A delay of roughly 70 ms was observed between the change in membrane voltage and the change in scattering intensity (Fig. 6). Ongoing research is investigating possible sources of this delay. Possible contributions include the separation between the site of the electrode tip placement and where optical recordings were made, slow conduction velocity of the action potential due to poor condition of the neuron, or the time required for the neuron to dynamically change the optical scattering properties of the membrane. Conduction velocities of roughly 5 mm/s have been reported in *Aplysia* bag cell neurons [22]. Assuming a propagation distance of roughly 50 microns this would result in a delay of 10 ms. A slower conduction velocity could be explained by poor health of the neuron or iatrogenic injury by the stimulating/recording electrode. Conduction velocities of *Aplysia* neurons can also vary depending on the state of the animal from which the neurons are harvested [23]. Despite the

delay, the changes in scattering that were observed have the same duration and are proportional to the induced electrical activity.

A major challenge for using OCT and OCM for detecting neural activity is that the intrinsic optical signals are small and are accompanied by signals from many sources of noise. Fluctuations in scattering intensity were observed from cultured bag cell neurons in their resting state. This effect was less evident in the OCT imaging of the intact ganglion, possibly due to spatially averaging of the fluctuations as a result of the lower transverse resolution. The fluctuations in scattering in the cultured bag cells decreased dramatically when they were treated with isotonic potassium chloride (KCl), leading us to believe they are associated with the functional activity of the neurons. Adding KCl to the culture media eliminates the electrochemical gradient that exists across the membranes, effectively killing the neurons. Possible physiological mechanisms of fluctuations in scattering include trafficking of vesicles in the cytoplasm or cytoplasmic streaming. The mechanisms from non-excited neurons are being investigated, and may result in a means for non-invasively determining other forms of functional neuron activity or processes. Since these fluctuations are not correlated to the induced electrical activity, a low amount of signal averaging was needed to identify the changes associated with action potentials. This averaging, however, is consistent with other electrophysiological studies.

Future improvements in detection sensitivity could be achieved using variations of OCT and OCM. Polarization-sensitive OCT (PS-OCT) is an imaging technique that enables depth-resolved mapping of the birefringence of biological tissue [24]. Changes in the birefringence of nerves due to electrical activity have been shown to be an order of magnitude larger than scattering intensity changes [5]. PS-OCT requires relatively minor changes to a typical OCT system, thus it could potentially provide significant improvements in sensitivity with little additional instrumentation. Phase-sensitive interferometric techniques have been used to measure nerve displacements less than 1 nm [12]. OCT is capable of phase-resolved imaging [25] which could also potentially be used to improve detection sensitivity of scattering changes from individual neurons or sparse populations of neurons. Combinations of phase-resolved and polarization-sensitive OCT are possible [26] and may ultimately result in the highest detection sensitivity. Other possible improvements include faster imaging speed. In this study, optical scattering changes from a single position of the beam were recorded. However, line rates of several hundreds of kilohertz have been reported for OCT [27], meaning that 2D cross-sectional images could potentially be acquired at frame rates fast enough to detect most electrical activity in neural tissue. Additional investigations are needed to determine how effectively these intrinsic optical signals can be recorded from individual neurons from other species. For example, single mammalian hippocampal neurons are smaller (< 10 microns in diameter), have faster action potentials (~1 ms) with faster propagation velocities (> 10 m/s), and will likely generate intrinsic optical scattering signals that are lower in magnitude.

## Conclusions

In summary, we show that optical coherence imaging can be used to detect changes in the scattering intensity from single neurons during action potentials. OCT allows depth-resolved changes to be observed over a long depth-of-field. OCM provides a higher transverse resolution but a reduced depth-of-field. Correlations between membrane voltage and scattering intensity from single neurons show that changes in optical scattering on the same time scale as action potentials can be detected. These results suggest that optical coherence imaging has potential use in neuroscience for non-invasively detecting neural activity in single neurons without the use of electrodes or fluorescent labels.

## Acknowledgements

The authors would like to thank Dr. Xiaoying Ye, Dr. Stanislav Rubakhin, and Prof. Jonathan Sweedler from the Beckman Institute for Advanced Science and Technology for assisting in the dissection and culturing of the specimens. This research was supported in part from grants

from the National Science Foundation (BES 03-47747, S.A.B.) and the National Institutes of Health (NIBIB, R01 EB005221, S.A.B.). Additional information can be found at <http://biophotonics.illinois.edu>.